

Proprioceptive Robot Collision Detection through Gaussian Process Regression

Alberto Dalla Libera¹, Elisa Tosello¹, Gianluigi Pillonetto¹, Stefano Ghidoni¹ and Ruggero Carli¹

Abstract— This paper proposes a proprioceptive collision detection algorithm based on Gaussian Regression. Compared to sensor-based collision detection and other proprioceptive algorithms, the proposed approach has minimal sensing requirements, since only the currents and the joint configurations are needed. The algorithm extends the standard Gaussian Process models adopted in learning the robot inverse dynamics, using a more rich set of input locations and an ad-hoc kernel structure to model the complex and non-linear behaviors due to frictions in *quasi-static* configurations. Tests performed on a Universal Robots UR10 show the effectiveness of the proposed algorithm to detect when a collision has occurred.

I. INTRODUCTION

Collaborative Robotics has attracted an increasing interest over the last decade in the research community, mainly due to the fact that the design of robots able to collaborate with humans might have a great impact in several domains.

Human-robot collaboration is a challenging topic under different points of view but, likely, the most critical aspects are related to safety. Indeed, when robots and humans work side-by-side, they need to share their workspace, and, in these circumstances, robots should avoid dangerous and unexpected collision with humans. Despite several motion planning algorithms have been proposed [3] in order to minimize the collision probability, it is impossible to reduce the collision risk to zero. Clearly, in this context it is fundamental that robots are provided with robust strategies that can promptly detect collisions. Moreover, once a collision has been detected, the robot has to classify such collision, in particular discriminating between intended and unintended contacts, and it has to react accordingly.

In order to detect the interaction with the external environment, robots might be endowed with specific sensors, like artificial skins or force-sensors. However, this approach might have some limitations. Indeed artificial skins do not provide information about the collision intensity [4], while six axis force-sensors are expensive and highly sensitive to environmental parameters like temperature and humidity.

A solution alternative to the use of additional sensors is proprioceptive collision detection (CD) [5]. Proprioceptive collision detection algorithms identify when an external force is applied using only proprioceptive sensors, namely joint torque sensors and current sensors, besides the joint coordinates. We refer the interested reader to [5] for an overview

of the main state of the art collision detection algorithms. All the proposed approaches require the definition of a monitoring signal $s(t)$ and a threshold σ_{CD} . The algorithms assume that a collision occurred when s exceeds σ_{CD} , see [6],[7], [8] and [9]. It is worth remarking that these class of solutions require an accurate knowledge of the robot dynamics model, since they assume to know both the kinetics and dynamics parameters. Typically the former parameters are known, while the latter ones are estimated resorting to Fisherian estimators [10].

In this paper, to detect if an interaction has occurred, we propose a novel approach based on the Gaussian Process Regression (GPR) framework. This approach has minimal sensing requirements, since it needs only to measure the joint coordinates and the motor currents. In this work we extend the GPR algorithms based on semi-parametric priors (i.e., composed by the sum of a parametric component and a non-parametric component) developed to learn the robot inverse dynamics [11], [12], [13]. Compared to the standard approach, our algorithm can efficiently deal also with *quasi-static* configurations, namely, when the robot is stuck or the joints' velocities are very low. Specifically, relying on an enlarged set of input features and designing proper kernel structure, our estimator can model the complex behaviors due to static frictions and kinetic frictions at low velocities.

The paper is organized as follows: in Section II we briefly review state of the art proprioceptive collision detection algorithms based on external torques estimation. In Section III we present our collision detection strategy, based on Gaussian Regression. In Section IV we introduce standard GPR techniques adopted in the learning of the robot inverse dynamics, highlighting via a numerical example the limitations of these approaches when used to detect collision in *quasi-static* configurations. Then, in Section V we formally describe our learning algorithm and in Section VI we show some numerical results obtained using a UR10 robot.

II. CD VIA MONITORING EXTERNAL TORQUES

In this section we describe a state of the art solution proposed to solve the CD problem, see [5]. When a collision occurs, an external force $F_{ext}(t)$ is applied to the robot, and consequently the joints are subject to a torque $\tau_{ext}(t)$. Consider an n joints manipulator and let $q(t)$, $\dot{q}(t)$, $\ddot{q}(t)$ and $\tau_m(t) \in \mathbb{R}^n$, denote, respectively, the vectors of joints positions, velocities, accelerations and motor torques at time t ; in the following, to keep the notation compact, we point out explicitly the time dependence only when it is necessary.

¹A. Dalla Libera, E. Tosello, Gianluigi Pillonetto, S. Ghidoni and R. Carli are with the Department of Information Engineering, University of Padova, Via Gradenigo 6/B, 35131 Padova, Italy [dallaliber@dei.unipd.it, toselloe@dei.unipd.it, giapi@dei.unipd.it, ghidoni@dei.unipd.it, carlirug@dei.unipd.it]

The expression of τ_{ext} is given by

$$\tau_{ext} = M(\mathbf{q})\ddot{\mathbf{q}} + C(\mathbf{q}, \dot{\mathbf{q}})\dot{\mathbf{q}} + \tau_g(\mathbf{q}) + \tau_\epsilon - \tau_m, \quad (1)$$

where $M(\mathbf{q}) \in \mathbb{R}^{n \times n}$ is the generalized inertia matrix, $C(\mathbf{q}, \dot{\mathbf{q}}) \in \mathbb{R}^{n \times n}$ is the Coriolis matrix, $\tau_g(\mathbf{q}) \in \mathbb{R}^n$ models the effects due to the gravitational force and $\tau_\epsilon \in \mathbb{R}^n$ describes the torques related to the unmodeled dynamic behaviors, mainly frictions and elasticity of the links [14].

Collision detection through direct monitoring of τ_{ext} defines $s(\mathbf{q}, \dot{\mathbf{q}}, \ddot{\mathbf{q}}, \tau_m) = \hat{\tau}_{ext}(\mathbf{q}, \dot{\mathbf{q}}, \ddot{\mathbf{q}}, \tau_m)$, where $\hat{\tau}_{ext}$ is the estimate of τ_{ext} obtained from equation (1) considering $\tau_\epsilon = 0$; given measurements of \mathbf{q} , $\dot{\mathbf{q}}$, $\ddot{\mathbf{q}}$ and τ_m we have

$$\hat{\tau}_{ext} = M(\mathbf{q})\ddot{\mathbf{q}} + C(\mathbf{q}, \dot{\mathbf{q}})\dot{\mathbf{q}} + \tau_g(\mathbf{q}) - \tau_m. \quad (2)$$

Ideally we should have $s(\cdot) = 0$ when $\tau_{ext} = 0$; in practice, given the model inaccuracies and the measurement noise, it happens that the monitoring signal is different from zero even when no external forces are applied. Consequently the introduction of a threshold σ_{CD} is necessary, and the binary collision function $f_{CD}(\cdot)$ is defined as

$$f_{CD}(s) = \begin{cases} \text{TRUE}, & \text{if } |s| \geq \sigma_{CD} \\ \text{FALSE}, & \text{if } |s| < \sigma_{CD} \end{cases},$$

where $|\cdot|$, \geq and $<$ are element wise operators, and $|s| \geq \sigma_{CD}$ if the relation holds at least for one component. The value of σ_{CD} is set by cross validation with the purpose of limiting the number of false positives and false negatives. Typically the identification of σ_{CD} is done observing the evolution of $s(\cdot)$ obtained while the robot is moving with $\tau_{ext} = 0$ for a time interval sufficiently large from the statistical point of view, see for examples [5].

Finally observe that, in the computation of $\hat{\tau}_{ext}$ in (2), it is assumed to know the model of the robotic arm, that is defined by kinematic parameters and dynamics parameters. Typically kinematic parameters are known while dynamics parameters are estimated by resorting to some Fisherian approach [10].

III. GPR FOR PROPRIOCEPTIVE COLLISION DETECTION

In this paper, we propose a novel approach based on the GPR framework to solve the CD problem. In particular a GPR-based method is used to build the monitoring signal s . In the following, instead of measuring directly the torque τ_m , we assume to measure the current i of the motors generating the torque τ_m applied to the joints; this is due to the fact that in our experimental setup we have access to i and not to τ_m . However, it is worth stressing that a current-based approach has minimal requirements as far as the number of sensors employed is concerned.

To consider the motor currents i instead of τ_m , we need to include the mechanical equations of the motors in the robotic arm model. Let $\theta(t)$, $\dot{\theta}(t)$ and $\ddot{\theta}(t)$ be the angular position, velocity and acceleration of the motors; then the mechanical equations of the motors are

$$J_m\ddot{\theta} + B_m\dot{\theta} - K_\tau i = \tau_L, \quad (3)$$

where τ_L are the torques due to the load, and J_m , B_m and $K_\tau \in \mathbb{R}^{n \times n}$ are diagonal matrices containing respectively the rotor inertias, the motors damping coefficient and

the torques-current ratios. When the behaviors due to the elasticity of the gears are negligible and $\tau_{ext} = 0$ it holds $\dot{\theta} = K_r\dot{\mathbf{q}}$, $\ddot{\theta} = K_r\ddot{\mathbf{q}}$ and $\tau_L = K_r^{-1}\tau_m$, with $K_r \in \mathbb{R}^{n \times n}$ equals to the diagonal matrix containing the gear reduction ratios. Substituting these equations in (3), we can express τ_m as function of \mathbf{q} , $\dot{\mathbf{q}}$, $\ddot{\mathbf{q}}$ and i , and equation (1) becomes:

$$M_{eq}(\mathbf{q})\ddot{\mathbf{q}} + C(\mathbf{q}, \dot{\mathbf{q}})\dot{\mathbf{q}} + \tau_g(\mathbf{q}) + \tau_\epsilon + B_{eq}\dot{\mathbf{q}} = K_{eq}i, \quad (4)$$

where for compactness we defined $M_{eq}(\mathbf{q}) = M(\mathbf{q}) + K_r^2 J_m$, $B_{eq} = K_r^2 B_m$ and $K_{eq} = K_r K_\tau$.

Instead of estimating τ_{ext} directly from (1), we propose to learn a GPR model that provides an estimate of i , denoted as \hat{i} , when τ_{ext} is null, i.e., $\tau_{ext} = 0$; more specifically we train a suitable GPR model for i , over a sufficiently rich dataset containing only trajectories obtained with $\tau_{ext} = 0$. Then the monitoring signal s is defined as the difference between the measured current i and \hat{i} . Clearly, if no collision has occurred, i.e., τ_{ext} is effectively null, then we expect \hat{i} to be close to i and, in turn, s to be small; viceversa if a collision has happened, i.e., $\tau_{ext} \neq 0$, then \hat{i} should be significantly different from i and s should become sufficiently large to detect the contact.

We stress the fact that in this paper we focus only on the development of GPR models able to produce proper monitoring signals while we do not discuss any strategy to design the threshold σ_{CD} . However σ_{CD} might be set using standard rules [5], like cross-validation.

IV. GPR FOR ROBOT INVERSE DYNAMICS

In this Section we briefly introduce the GPR framework [15], focusing in the standard models used in the learning of the inverse dynamics, [11],[12],[13].

Let \mathbf{y} be a vector of measurements and let $X = \{\mathbf{x}_1, \dots, \mathbf{x}_N\}$ be the set of the corresponding input locations, with $\mathbf{x}_k \in \mathbb{R}^p$, the probabilistic model of GPR is

$$\mathbf{y} = \begin{bmatrix} y_1 \\ \vdots \\ y_N \end{bmatrix} = \begin{bmatrix} f(\mathbf{x}_1) \\ \vdots \\ f(\mathbf{x}_N) \end{bmatrix} + \begin{bmatrix} e_1 \\ \vdots \\ e_N \end{bmatrix} = f(X) + e(X) \quad (5)$$

where e is Gaussian i.i.d. noise with covariance σ_e and $f(\mathbf{x}_k) : \mathbb{R}^p \rightarrow \mathbb{R}$ is an unknown function defined as a Gaussian Process, namely $f(X) \sim N(\mathbf{m}_f(X), K(X, X))$, where $\mathbf{m}_f(X)$ is the mean of the process and $K(X, X)$ is the corresponding covariance. Typically $K(X, X)$ is named kernel matrix and it can be defined through a kernel function $k(\mathbf{x}_i, \mathbf{x}_j)$, i.e. the $K(X, X)$ entry in i -th row and j -th column is equal to $k(\mathbf{x}_i, \mathbf{x}_j)$. Under these assumptions the posterior probability of \mathbf{f} is Gaussian and then $\hat{\mathbf{f}}$, the maximum a posteriori estimation of \mathbf{f} , is the mean of the \mathbf{f} posterior distribution.

A. GPR robot inverse dynamics

The robot inverse dynamics problem consists in learning the function f that maps \mathbf{q} , $\dot{\mathbf{q}}$ and $\ddot{\mathbf{q}}$ in τ_m . Typically GPR approaches consider each joint ℓ as stand-alone. Referring to the notation introduced in (5), for each joint ℓ we introduce a GPR model $y_k = f_\ell(\mathbf{x}_k) + e_k$, where

$\mathbf{x}_k = [\mathbf{q}(t_k), \dot{\mathbf{q}}(t_k), \ddot{\mathbf{q}}(t_k)]$, $y_k = \tau_{m_\ell}(\mathbf{x}_k)$ and where the ℓ subscript denotes that measurement is referred to the ℓ -th link. Since in our setup we consider currents instead of torques we have $y_k = i_\ell(\mathbf{x}_k)$.

The most crucial aspect in GPR is related to the choice of the prior distribution of $f_\ell(\cdot)$, i.e. the selection of good $m_{f_\ell}(\cdot)$ and $k_\ell(\cdot, \cdot)$. The different priors adopted in Robotics can be grouped in three families, in particular, parametric priors (PPs), non-parametric priors (NPPs) and semi-parametric priors (SPPs).

1) *Parametric priors*: When equation (1) is given, it is possible to derive an expression of $m_{f_\ell}(\cdot)$ and $k_\ell(\cdot, \cdot)$ which is inspired by the model. Indeed, in [14], it has been shown that the dynamic model in (1) can be rewritten, when neglecting the unmodeled effects, i.e., assuming $\tau_\epsilon = 0$, as a linear time-variant model. Formally, when $\tau_{ext} = 0$ it holds:

$$\boldsymbol{\tau}_m = \begin{bmatrix} \tau_{m_1} \\ \vdots \\ \tau_{m_n} \end{bmatrix} = \begin{bmatrix} \phi_1^d(\mathbf{q}, \dot{\mathbf{q}}, \ddot{\mathbf{q}}) \\ \vdots \\ \phi_n^d(\mathbf{q}, \dot{\mathbf{q}}, \ddot{\mathbf{q}}) \end{bmatrix} \mathbf{w}_d = \Phi^d(\mathbf{q}, \dot{\mathbf{q}}, \ddot{\mathbf{q}}) \mathbf{w}_d, \quad (6)$$

where $\mathbf{w}_d \in \mathbb{R}^m$ denotes the vector casting together all the dynamic parameters of the robot. The same property holds also if we consider i instead of τ_m , i.e. equation (4) instead of (1).

Then, considering $f_\ell(\mathbf{x}_k) = \phi_\ell^d(\mathbf{x}_k) \mathbf{w}_d$ with $\mathbf{w}_d \sim N(\mathbf{m}_{\mathbf{w}_d}, \Sigma_{\mathbf{w}_d})$, we have

$$f_\ell(X) \sim N\left(\Phi_\ell^d(X) \mathbf{w}_d, \Phi_\ell^d(X) \Sigma_{\mathbf{w}_d} \Phi_\ell^d(X)^T\right),$$

with $\Phi_\ell^d(X) \in \mathbb{R}^{N \times m}$ obtained casting together the vectors $\phi_\ell^d(\cdot)$ evaluated in the input locations of X . The kernel function of the process is $k_\ell(\mathbf{x}_i, \mathbf{x}_j) = \phi_\ell^d(\mathbf{x}_i) \Sigma_{\mathbf{w}_d} \phi_\ell^d(\mathbf{x}_j)^T$, and it is equivalent to a linear kernel. The mean function is $m_{f_\ell}(\mathbf{x}_k) = \phi_\ell^d(\mathbf{x}_k) \mathbf{m}_{\mathbf{w}_d}$.

A refinement of this model can be obtained including also some terms modeling the frictions effects. The simplest and most used model to describe the torque applied to the ℓ -th joint by frictions, denoted as τ_{f_ℓ} , is given by

$$\tau_{f_\ell}(t) = \begin{cases} \tau_{m_\ell}(t) & \text{if } \dot{q}_\ell(t) = 0, \tau_{f_\ell}(t) \leq F_{s_\ell} \\ F_{k_\ell} \text{sign}(\dot{q}_\ell(t)) + F_{v_\ell} \dot{q}_\ell(t) & \text{if } |\dot{q}_\ell(t)| > 0 \end{cases} \quad (7)$$

where F_{s_ℓ} , F_{k_ℓ} and F_{v_ℓ} are respectively the static friction coefficient, the kinetic friction coefficient and the viscous friction coefficient of the ℓ -th joint [16]. Notice that when \dot{q}_ℓ is not null τ_{f_ℓ} is linear respect to F_{k_ℓ} and F_{v_ℓ} and hence the behaviors due to the kinetic frictions can be easily merged in (6) leading to the augmented equation

$$\tau_{m_\ell}(\mathbf{x}_k) = \begin{bmatrix} \phi_\ell^d(\mathbf{x}_k) & \phi_\ell^f(\mathbf{x}_k) \end{bmatrix} \begin{bmatrix} \mathbf{w}_d \\ \mathbf{w}_{f_\ell} \end{bmatrix} := \phi_\ell(\mathbf{x}_k) \mathbf{w}_\ell \quad (8)$$

where $\phi_\ell^f(\mathbf{x}_k) = [\text{sign}(\dot{q}_\ell) \quad \dot{q}_\ell]$ and $\mathbf{w}_{f_\ell} = [F_{k_\ell} \quad F_{v_\ell}]^T$.

2) *Non-Parametric priors*: When no prior knowledge about the process is available, the most common choice is to consider $m_{f_\ell}(\cdot) = 0$ and define $K_\ell(X, X)$ directly through a kernel function $k_\ell(\cdot, \cdot)$. The most used kernel in robotic identification is the Radial Basis Kernel (RBK), defined as

$$k_{RBK}(\mathbf{x}_i, \mathbf{x}_j) = \lambda \exp\left(-\frac{(\mathbf{x}_i - \mathbf{x}_j)^T \Sigma_{RBK}^{-1} (\mathbf{x}_i - \mathbf{x}_j)}{2}\right) \quad (9)$$

where Σ_{RBK} is typically a diagonal matrix, whose diagonal elements σ_{RBK} are referred to as length-scales.

3) *Semi-Parametric priors*: The semi-parametric approach models the function $f_\ell(\cdot)$ as the sum of two independent contributions, a parametric component $f_{P_\ell} = \phi_\ell^d(\mathbf{x}_k) \mathbf{w}_d$ and a non-parametric component $f_{NP_\ell}(\cdot)$, for example defined by an RBK i.e. $f_\ell(\mathbf{x}_k) = \phi_\ell^d(\mathbf{x}_k) \mathbf{w}_d + f_{NP_\ell}(\mathbf{x}_k)$. Typically, there are two ways to include the parametric component. (i) Assuming that \mathbf{w}_d is a deterministic variable, eventually pre-trained adopting a parametric-based estimator; in this case the mean and the kernel of $f_\ell(\cdot)$ is $m_{f_\ell}(\mathbf{x}_k) = \phi_\ell^d(\mathbf{x}_k) \mathbf{w}_d$ and $k_\ell(\mathbf{x}_i, \mathbf{x}_j) = k_{RBK}(\mathbf{x}_i, \mathbf{x}_j)$. (ii) Assuming that \mathbf{w}_d is a random variable independent from $f_{NP_\ell}(\cdot)$, thus obtaining $m_{f_\ell}(\mathbf{x}_k) = \phi_\ell^d(\mathbf{x}_k) \mathbf{m}_{\mathbf{w}_d}$ and $k_\ell(\mathbf{x}_i, \mathbf{x}_j) = \phi_\ell^d(\mathbf{x}_i) \Sigma_{\mathbf{w}_d} \phi_\ell^d(\mathbf{x}_j)^T + k_{RBK}(\mathbf{x}_i, \mathbf{x}_j)$.

B. Limitations of proprioceptive collision detection with standard GPR approach

In this subsection we discuss a simple experiment that highlights the limitations of these standard GPR estimators when working in the *quasi-static* configurations. The experiment, reported in Figure 1, consists in a succession of rest phases (all the joints stuck and parallel to the ground) and moving phases. In the moving phases only the first joint is actuated, such that the values of q_1 in the rest phase are sequentially $\frac{\pi}{2}$, 2.09 , $\frac{\pi}{2}$, 0.52 [rad].

In Figure 1, the blue line represents the monitoring signal s_{SP_S} obtained estimating the current using a standard semi-parametric estimator. Notice that, while during the moving phases the frequency of s_{SP_S} is particularly high and it might be easily canceled with a low pass filter, during the rest phases s_{SP_S} is significantly greater than zero for sufficiently long intervals. Consequently a collision might be detected, generating a false positive.

This fact is caused by the poor estimation performances of the standard GPR estimators when the robot is in *quasi-static* configurations (see results in Section VI-A). Indeed at low velocities the forces due to frictions are more relevant and particularly unpredictable [16]. As confirmed by equation (8), when $|\dot{q}_\ell| < \sigma_v$ the model is highly non linear and strongly dependent on different factors like the physical properties of the materials. The threshold σ_v defines the transition between *dynamical* and *quasi-static* configurations. Its value can be validated via cross-correlation and in this paper it has been set equal to 10^{-2} . See [17] for details.

This experiment shows another interesting fact explaining the reason why the non-parametric component is not able to capture the behaviors due to τ_f when $|\dot{q}| < \sigma_v$. Observe that in the rest phases with $q_1 = \pi/2$, despite the robot is in the same configuration \mathbf{x}_q , the current i_1 assumes three different values. Referring to the GPR notation, the function $f_1(\cdot)$ attains different values in the same input location \mathbf{x}_q , and the difference among these values is so significant that can not be explained by only the presence of noise in the measurements. Similar situation happens in linear classification, when two classes are not linearly separable, and it denotes the need of more input features.

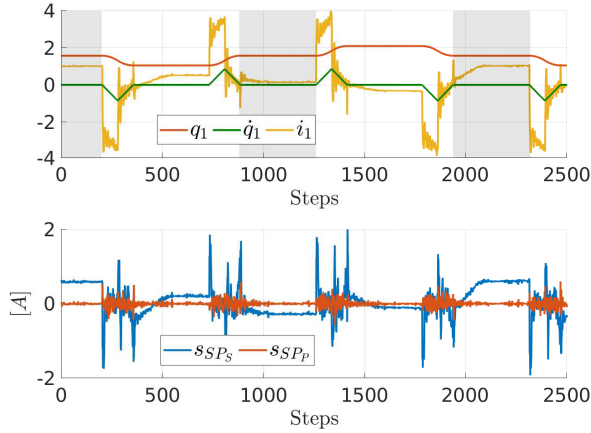


Fig. 1: Cyclic actuation of the first link. s_{SP_s} and s_{SP_p} denote the monitoring signals obtained, respectively, by a standard semi-parametric estimator and the proposed approach.

V. PROPOSED LEARNING ALGORITHM

The proposed solution is based on the following observations. (i) Experimental results in Section VI-A show that, when working in a *dynamical* configuration, a semi-parametric kernel provides accurate estimates when describing the input locations by the standard features \mathbf{q} , $\dot{\mathbf{q}}$, $\ddot{\mathbf{q}}$. (ii) When dealing with the *quasi-static* configuration, we need to include additional features in the input space, in order to avoid that the same input is mapped into different output. (iii) We need to model the discontinuity due to the different behaviors of static frictions and kinetic frictions, i.e., we need to provide a unified framework capturing the behaviors in both scenarios, *dynamical* and *quasi-static*.

Based on the above observations the learning algorithm we propose models the function f_ℓ adopting a semi-parametric model, where the parametric component f_{P_ℓ} includes also the frictions effects and where the non-parametric component f_{NP_ℓ} is given by the sum of two contributions; the first one trying to compensate the model inaccuracies and the second one capturing the discontinuous behaviors generated by the frictions in the transition intervals between static and dynamic frictions.

Before formally describing the model we consider, we provide some more details about the second and third observation above.

A. Additional features

Notice, from Equation (7), that when the velocity is null, important contributions are given by τ_m , that is a term related to the action of the controller. Consequently in *quasi-static* configurations it might be necessary to add to the GPR inputs some features related to the control actions. We stress the fact that, from a control point of view, we are operating in a black box context since we do not have access to the low level controller of the UR robot we used in our experiments.

In our learning algorithm, when dealing with the *quasi-static* case, the input locations are described by the following

augmented features vector,

$$\mathbf{x}_k^a = [\mathbf{q}(t_k), \dot{\mathbf{q}}(t_k), \ddot{\mathbf{q}}(t_k), \mathbf{e}_q(t_k), \dot{\mathbf{e}}_q(t_k), \mathbf{i}_c(t_k)] \quad (10)$$

where $\mathbf{e}_q(t_k)$ and $\dot{\mathbf{e}}_q(t_k)$ denote, respectively, the joint position and velocity errors at time t_k , while $\mathbf{i}_c(t_k)$ are the currents required by the controllers of the motors at the instant t_k .

The rationale behind the choice of adopting this set of features is the following: the variables \mathbf{e}_q and $\dot{\mathbf{e}}_q$ allow to model proportional and derivative contributions while the \mathbf{i}_c bring information about non linear control actions (i.e. saturation) and dynamic contribution (i.e. integral contribution).

B. Modeling of friction discontinuity through NPP

In our approach, to capture the discontinuity between static frictions and kinematic frictions we add to our model a non-parametric component. In the following, to keep compact the description of our model, we exploit two properties of kernels functions [15]. (i) The sum of kernels is a kernel. (ii) Vertical rescaling: let $k(\cdot, \cdot)$ be the kernel function of the Gaussian Process $f(\mathbf{x}_k)$ and $a(\mathbf{x}_k)$ a deterministic function. Then $a(\mathbf{x}_i)k(\mathbf{x}_i, \mathbf{x}_j)a(\mathbf{x}_j)$ is a valid kernel function and in particular it is associated to the process $a(\mathbf{x}_k)f(\mathbf{x}_k)$.

The non-parametric component f_{NP_ℓ} of our model is given as the sum of two Gaussian Processes, $f_{NP_{\ell;stc}}(\cdot)$ and $f_{NP_{\ell;kin}}(\cdot)$, where the first one is scaled by the function

$$a_\ell(\mathbf{x}_k^a) = \begin{cases} 0 & \text{if } |\dot{q}_{k_\ell}| \geq \sigma_v \\ 1 & \text{if } |\dot{q}_{k_\ell}| < \sigma_v \end{cases}.$$

It turns out that

$$f_{NP_\ell}(\mathbf{x}_k^a) = a_\ell(\mathbf{x}_k^a)f_{NP_{\ell;stc}}(\mathbf{x}_k^a) + f_{NP_{\ell;kin}}(\mathbf{x}_k). \quad (11)$$

The first component (that is a function of the augmented input vector \mathbf{x}_k^a), acts only when the ℓ -th link is in *quasi-static* configurations, with the specific task of capturing the behaviors due to frictions at low velocity. Instead $f_{NP_{\ell;kin}}$ tries to compensate for the PP inaccuracies, and it is active on both the *dynamical* and *quasi-static* configurations; for this reason it depends only on \mathbf{q} , $\dot{\mathbf{q}}$, $\ddot{\mathbf{q}}$ and not on the additional features $\mathbf{e}_q, \dot{\mathbf{e}}_q, \mathbf{i}_c$ ¹

C. Proposed Algorithm

The proposed learning algorithm is based on a semi-parametric model described by the following expression

$$f_\ell(\mathbf{x}_k^a) = \bar{\phi}_\ell(\mathbf{x}_k)\mathbf{w}_\ell + a_\ell(\mathbf{x}_k)f_{NP_{\ell;stc}}(\mathbf{x}_k^a) + f_{NP_{\ell;kin}}(\mathbf{x}_k), \quad (12)$$

where $\bar{\phi}_\ell(\cdot)$ is defined as $\phi_\ell(\cdot)$, except that the contributions of $\phi_\ell^f(\cdot)$ are nulled when $|\dot{q}_\ell| < \sigma_v$. This choice is motivated by the experimental evidence that shows how the linear model is not accurate in *quasi-static* configurations.

In our implementation the information coming from the parametric contribution is added considering \mathbf{w}_ℓ as a deterministic value, i.e. influencing only the mean of $f_\ell(\cdot)$. As far

¹Formally, in (11), $f_{NP_{\ell;kin}}$ should depend on \mathbf{x}_k^a . However, based on the observation reported, we have made explicit the fact that the additional features do not affect the value of $f_{NP_{\ell;kin}}$ which depends only on the standard features $\mathbf{x}_k = (\mathbf{q}(t_k), \dot{\mathbf{q}}(t_k), \ddot{\mathbf{q}}(t_k))$.

as the $f_{NP_{\ell,static}}$ and $f_{NP_{\ell,kin}}$ components are concerned, we defined them adopting RBK kernels with ARD.

VI. EXPERIMENTS

A Universal Robots UR10² is used for the experiments. It is a collaborative industrial robot with 6-degrees of freedom. The interface with the UR10 is based on ROS (Robot Operating System, [18]), through the *ur_modern_driver*³. Data are acquired with a sampling time of $8 \cdot 10^{-3}sec$. The data processing and the derivation of the physical model are implemented in MATLAB, while the GPR in Python, in order to exploit the PyTorch computational advantages during the model optimization [19].

The normalized mean squared error (nMSE) between i and \hat{i} has been considered in order to evaluate the algorithms accuracy,

$$nMSE(X) = \frac{\sum_{k=1}^N (i_{\ell}(\mathbf{x}_k) - \hat{i}_{\ell}(\mathbf{x}_k))^2 / N}{Var(i_{\ell}(X_*))}, \quad (13)$$

The algorithms tested are P_f , a PP-based estimator with linear features modeling kinetic frictions, SP_S , a SPP-based estimator with standard input features and SP_P , the proposed approach.

A. Random exploration of the workspace

In this experiment we test the estimation performances of the learning algorithms, stressing the generalization properties. We considered two data sets. The first is pointed by D_1 , and it consist in a set of trajectories collected requiring to the end-effector to reach 200 random points (for a total of 80000 input locations) randomly distributed within an hemisphere of the robot workspace. The other data set D_2 is composed by 22000 data points collected requiring the robot to reach 50 random points inside the previous hemisphere and to track a circle of radius 30[cm] at a tool speed of 30[mm/s]. The algorithms have been trained minimizing the negative marginal log likelihood (MLL) over D_1 . Given the number of samples, to minimize the negative MLL we resorted to stochastic gradient descent [20], in particular we adopted the ADAM optimizer [21]. Furthermore, once the hyperparameters have been selected, we down-sampled the training set to obtain D_{SDP} , a subset of data points with 5000 samples, used to derive the estimation; the set composed by the remaining input locations is $D_{1_{test}}$. The performances over $D_{1_{test}}$ compare the estimators accuracy in points that are close to D_{SDP} , i.e. in points that are close to the input locations used to derive the model. In contrast D_2 is thought to stress the estimators generalization properties, and might contains input locations that are far from the ones in D_{SDP} .

Results reported in Figure 2 show that when links are in non static configurations, namely, when $|\dot{q}_{\ell}| > \sigma_v$, performances of all the estimators are comparable. This is related to the fact that in these configurations the parametric contributions can capture a relevant part of the signal.

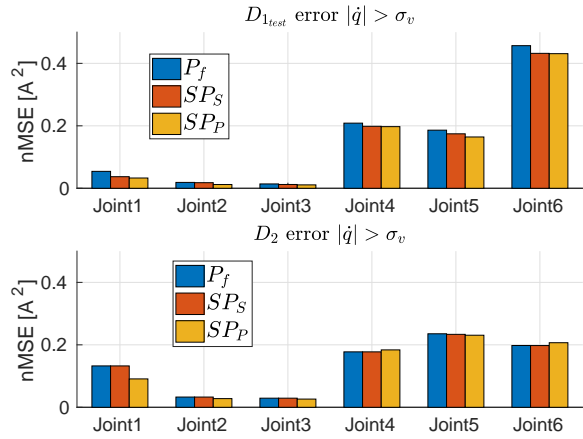


Fig. 2: Bar-plot of the nMSE in dynamical configurations.

Comparing the nMSE of SP_S and P_f , we can appreciate that the addition of the NP contribution in SP_S allows to improve the accuracy in points that are close to $D_{1_{SDP}}$, since SP_S over-performs P_f in $D_{1_{test}}$. However the NP contribution tends to vanish when SP_S is tested in D_2 .

In dynamical configurations the proposed approach behaves similarly to SP_S . However notice that in joint 1 and 2 SP_P significantly improves the P_f performances, even in D_2 . This aspect suggests that the ad-hoc kernel structure proposed in (11) entails advantages also in the dynamical configurations.

The nMSEs in the static and quasi-static configurations are reported in Figure 3. The bar-plot highlights that in these configurations P_f does not capture relevant components of the output signal, except for joint 2 and 3. Indeed in link 2 and 3 when the robot is in static configurations the gravitational contributions are predominant, and P_f is able to capture them.

The nMSE index for SP_S highlights how the NP contribution in SP_S is extremely local, since it reduces considerably the nMSE only over $D_{1_{test}}$. Moreover, the SP_S performance over D_2 suggests that the semi-parametric estimator with standard inputs is subject to overfitting, give that its nMSE is greater that the one of P_f .

The SP_P estimator instead exhibits good performances in static and quasi-static configurations over both the datasets, suggesting that the additional features, together with the ad-hoc kernel structure are crucial to model the complex behaviors generated by static frictions.

B. Detection of human-robot interaction

In order to validate the CD algorithm proposed, we applied SP_P on a real test case: the detection of human-robot interaction. We tested the algorithm both in dynamical and quasi-static configurations. In the first part of the experiment the end-effector of the robot is tracking a circle, while in the last part it stays in the final configuration. A human user applies an external force to the first robot joint four times, two during the moving phase and two during the quasi-

²www.universal-robots.com/UR10

³https://github.com/ThomasTimm/ur_modern_driver

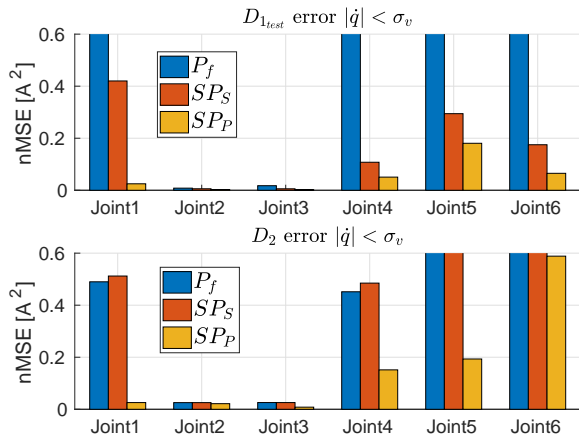


Fig. 3: Bar-plot of the nMSE in *quasi-static* configurations.

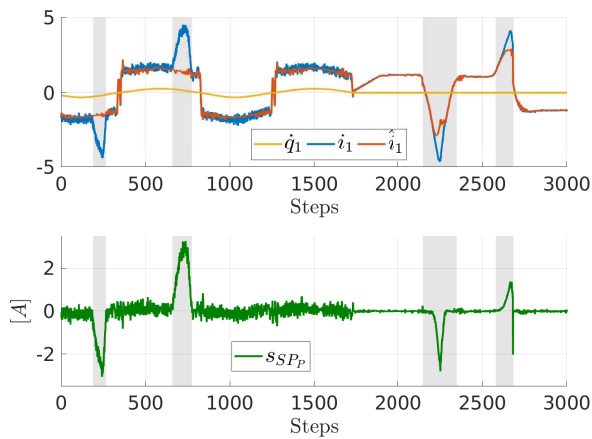


Fig. 4: Evolution of i_1 , \hat{i}_1 , \dot{q}_1 and s_{SP_P} when external forces are applied to the first link of the UR10. The gray bars indicates the interval in which the interactions occurred.

static phase⁴. The SP_P estimator is the same of Experiment VI-A, derived starting from the D_{SDP} data. The experiment is described in Figure 4. The gray bar highlights the time intervals in which the interactions occurred. The results show that SP_P can be exploited to define a good monitoring signal. Indeed the prediction error s_{SP_P} is significantly not null only when the external forces are applied, allowing the detection of the interactions, and at the same time avoiding the possibility of incurring in false positives.

VII. CONCLUSIONS

In this paper we validated the use of GPR to solve the proprioceptive collision detection problem, focusing on the definition of a good monitoring signal. The proposed approach has minimal requirements in terms of sensors, since only joint coordinates and motor currents are needed. The proposed monitoring signal corresponds to the estimate of the currents due to external torques. In particular we focused on the behaviors of the monitoring signal in static

and *quasi-static* configurations, that are particularly relevant in collaborative robotics. The proposed approach has been tested in a UR10. The experimental results prove the validity of these methods.

REFERENCES

- [1] G. J. Gelderblom, M. D. Wilt, G. Cremers, and A. Rensma, “Rehabilitation robotics in robotics for healthcare; a roadmap study for the european commission,” in *2009 IEEE International Conference on Rehabilitation Robotics*, June 2009, pp. 834–838.
- [2] P. Masinga, H. Campbell, and J. A. Trimble, “A framework for human collaborative robots, operations in south african automotive industry,” in *2015 IEEE International Conference on Industrial Engineering and Engineering Management (IEEM)*, Dec 2015, pp. 1494–1497.
- [3] D. M. Ebert and D. D. Henrich, “Safe human-robot-cooperation: image-based collision detection for industrial robots,” in *IEEE/RSJ International Conference on Intelligent Robots and Systems*, vol. 2, Sept 2002, pp. 1826–1831 vol.2.
- [4] A. Cirillo, F. Ficuciello, C. Natale, S. Pirozzi, and L. Villani, “A conformable force/tactile skin for physical humanrobot interaction,” *IEEE Robotics and Automation Letters*, vol. 1, no. 1, pp. 41–48, Jan 2016.
- [5] S. Haddadin, A. D. Luca, and A. Albu-Schffer, “Robot collisions: A survey on detection, isolation, and identification,” *IEEE Transactions on Robotics*, vol. 33, no. 6, pp. 1292–1312, Dec 2017.
- [6] D. P. Le, J. Choi, and S. Kang, “External force estimation using joint torque sensors and its application to impedance control of a robot manipulator,” in *2013 13th International Conference on Control, Automation and Systems (ICCAS 2013)*, Oct 2013, pp. 1794–1798.
- [7] E. Villagrossi, “Robot dynamic modelling and control for machining applications,” Ph.D. dissertation, University degli Studi di Brescia, 2015.
- [8] A. D. Luca, A. Albu-Schaffer, S. Haddadin, and G. Hirzinger, “Collision detection and safe reaction with the dlr-iii lightweight manipulator arm,” in *2006 IEEE/RSJ International Conference on Intelligent Robots and Systems*, Oct 2006, pp. 1623–1630.
- [9] G. Doisy, “Sensorless collision detection and control by physical interaction for wheeled mobile robots,” in *2012 7th ACM/IEEE International Conference on Human-Robot Interaction (HRI)*, March 2012, pp. 121–122.
- [10] J. Wu, J. Wang, and Z. You, “An overview of dynamic parameter identification of robots,” *Robotics and Computer-Integrated Manufacturing*, vol. 26, no. 5, pp. 414 – 419, 2010.
- [11] J. Nakanishi, R. Cory, M. Mistry, J. Peters, and S. Schaal, “Operational space control: A theoretical and empirical comparison,” *International Journal of Robotics Research*, vol. 27, no. 6, pp. 737–757, Jun. 2008.
- [12] J.-A. Ting, M. Mistry, J. Peters, S. Schaal, and J. Nakanishi, “A bayesian approach to nonlinear parameter identification for rigid body dynamics,” in *RSS 2006*, Max-Planck-Gesellschaft. Cambridge, MA, USA: MIT Press, Apr. 2007, pp. 247–254.
- [13] D. Romeres, M. Zorzi, R. Camoriano, and A. Chiuso, “Online semi-parametric learning for inverse dynamics modeling,” in *2016 IEEE 55th Conference on Decision and Control (CDC)*, 2016.
- [14] B. Siciliano, L. Sciacivco, L. Villani, and G. Oriolo, *Robotics, Modelling, Planning and Control*, 2009.
- [15] C. E. Rasmussen, “Gaussian processes for machine learning.” MIT Press, 2006.
- [16] P. E. Dupont, “Friction modeling in dynamic robot simulation,” in *Robotics and Automation*, 1990.
- [17] N. D. Vuong and M. H. A. Jr, “Dynamic model identification for industrial robots,” in *IEEE Control Systems*, 2007.
- [18] M. Quigley, K. Conley, B. P. Gerkey, J. Faust, T. Foote, J. Leibs, R. Wheeler, and A. Y. Ng, “Ros: an open-source robot operating system,” in *ICRA Workshop on Open Source Software*, 2009.
- [19] A. Paszke, S. Gross, S. Chintala, G. Chanan, E. Yang, Z. DeVito, Z. Lin, A. Desmaison, L. Antiga, and A. Lerer, “Automatic differentiation in pytorch,” 2017.
- [20] G. E. Hinton, N. Srivastava, A. Krizhevsky, I. Sutskever, and R. R. Salakhutdinov, “Improving neural networks by preventing co-adaptation of feature detectors,” in <https://arxiv.org/abs/1207.0580>, 2012.
- [21] D. P. Kingma and J. L. Ba, “Adam : A method for stochastic optimization,” in *ICLR*, 2015.

⁴The experiment is visible at <https://youtu.be/2jJS8ajXhEw>